Research Article | Vol. 25, No. 9 | 1 May 2017 | OPTICS EXPRESS 9761

Optics EXPRESS

Group-velocity dispersion in SOI-based channel waveguides with reduced-height

RICCARDO MARCHETTI,[1,*] VALERIO VITALI,[1] COSIMO LACAVA,[1,2] ILARIA CRISTIANI,[1] BENOIT CHARBONNIER,[3] VIVIANE MUFFATO,[3] MARYSE FOURNIER,[3] AND PAOLO MINZIONI[1]

[1] *Integrated Photonics Lab, Department of Electrical, Computer, and Biomedical Engineering, University of Pavia, Via Ferrata, 5 A, I-27100 Pavia, Italy*
[2] *Optoelectronics Research Centre, University of Southampton, Southampton SO17 1BJ, UK*
[3] *Photonic Department, CEA MINATEC Campus, F-38054 Grenoble Cedex, France*
[*] *riccardo.marchetti02@universitadipavia.it*

Abstract: We report on the experimental characterization, in the telecom C-band, of group-velocity dispersion (D) in 100-nm high rectangular strip waveguides realized by silicon-on-insulator technology. We compare the experimental results with numerical predictions, showing that 100-nm high waveguides exhibit normal dispersion and that the absolute value of the dispersion coefficient D decreases as the waveguide width is increased. D at 1550 nm varies from -8130 to -3900 ps/(nm·km) by increasing the waveguide width from 500 to 800 nm.

OCIS codes: (130.0130) Integrated optics; (230.7370) Waveguides; (260.2030) Dispersion.

References and links

1. B. Jalali, and S. Fathpour, "Silicon photonics," J. Lightwave Technol. **24**(12), 4600–4615 (2006).
2. Q. Lin, O. J. Painter, and G. P. Agrawal, "Nonlinear optical phenomena in silicon waveguides: Modeling and applications," Opt. Express **15**(25), 16604–16644 (2007).
3. C. Lacava, M.A. Ettabib and P. Petropoulos, "Nonlinear silicon photonic signal processing devices for future optical networks," MDPI Appl. Sciences **7**(1), 103 (2017).
4. R. L. Espinola, J. I. Dadap, R. M. Osgood, Jr., S. J. McNab, and Y. A. Vlasov, "C-band wavelength conversion in silicon photonic wire waveguides," Opt. Express **13**(11), 4341–4349 (2005).
5. I-W. Hsieh, X. Chen, J. I. Dadap, N. C. Panoiu, R. M. Osgood, Jr., S. J. McNab, and Y. A. Vlasov, "Cross-phase modulation-induced spectral and temporal effects on co-propagating femtosecond pulses in silicon photonic wire," Opt. Express **15**(3), 1135–1146 (2007).
6. C. Ciret, F. Leo, B. Kuyken, G. Roelkens, and S. P. Gorza, "Observation of an optical event horizon in a silicon-on-insulator photonic wire waveguide," Opt. Express **24**(1), 114–124 (2016).
7. F. P. Payne, and J. P. R. Lacey, "A theoretical analysis of scattering loss from planar optical waveguide," Opt. Quantum. Electron. **26**(10), 977–986 (1994).
8. H. K. Tsang, C. S. Wong, T. K. Liang, I. E. Day, S. W. Roberts, A. Harpin, J. Drake, and M. Asghari, "Optical dispersion, two-photon absorption, and self-phase modulation in silicon waveguides at 1.5 μm wavelength," Appl. Phys. Lett. **80**(3), 416–418 (2002).
9. T. Barwicz, M. A. Popović, F. Gan, M. S. Dahlem, C. W. Holzwarth, P. T. Rakich, E. P. Ippen, F. X. Kärtner, and H. I. Smith, "Reconfigurable silicon photonic circuits for telecommunication applications," Proc. SPIE **6872**, 68720Z (2008).
10. T. Barwicz and H. A. Haus, "Three-dimensional analysis of scattering losses due to sidewall roughness in microphotonic waveguides," J. Lightwave Technol. **23**(9), 2719–2732 (2005).
11. M. A. Popović, T. Barwicz, M. S. Dahlem, F. Gan, C. W. Holzwarth, P. T. Rakich, H. I. Smith, E. P. Ippen, and F. X. Kärtner, "Tunable, fourth-order silicon microring-resonator add-drop filters," presented at the European Conference on Optical Communication, Berlin, Germany, Sept. 2007, paper 1.2.3.
12. M. S. Dahlem, C. W. Holzwarth, A. Khilo, F. X. Kärtner, H. I. Smith, and E. P. Ippen, "Reconfigurable multi-channel second-order silicon microring-resonator filterbanks for on-chip WDM systems," Opt. Express **19**(1), 306–316 (2011).
13. R. Marchetti, V. Vitali, C. Lacava, I. Cristiani, G. Giuliani, V. Muffato, M. Fournier, S. Abrate, R. Gaudino, E. Temporiti, L. Carroll and P. Minzioni "Low-loss micro-resonator filters fabricated in silicon by CMOS-compatible lithographic techniques: design and characterization," MDPI Appl. Sciences **7**(2), 174–185 (2017).
14. C. Lacava, R. Marchetti, V. Vitali, I. Cristiani, G. Giuliani, M. Fournier, S. Bernabe, and P. Minzioni, "Reduced nonlinearities in 100-nm high SOI waveguides," Proc. SPIE **9753**, 975313 (2016).

#286694 https://doi.org/10.1364/OE.25.009761
Journal © 2017 Received 13 Feb 2017; revised 17 Mar 2017; accepted 17 Mar 2017; published 19 Apr 2017

Optics EXPRESS

15. E. Dulkeith, F. Xia, L. Schares, W. M. J. Green, and Y. A. Vlasov, "Group index and group velocity dispersion in silicon-on-insulator photonic wires," Opt. Express **14**(9), 3853–3863 (2006).
16. A. C. Turner, C. Manolatou, B. S. Schmidt, M. Lipson, M. A. Foster, J. E. Sharping, and A. L. Gaeta, "Tailored anomalous group-velocity dispersion in silicon channel waveguides," Opt. Express **14**(10), 4357–4362 (2006).
17. L. Zhang, Q. Lin, Y. Yue, Y. Yan, R. G. Beausoleil, and A. E. Willner, "Silicon waveguide with four zero-dispersion wavelengths and its application in on-chip octave-spanning supercontinuum generation," Opt. Express **20**(2), 1685–1690 (2012).
18. L. Chrostowski, and M. Hochberg, *Silicon Photonics Design: From Devices to Systems* (Cambridge University, 2015).
19. P. Minzioni, G. Nava, I. Cristiani, W. Yan, and V. Degiorgio, "Wide-band single-shot measurement of refractive indices and birefringence of transparent materials," Optics & Laser Technology **50**, 71–77, (2013).

1. Introduction

In the last decade Silicon (Si) photonics established itself as a mature technology for the fabrication of miniaturized and cost-effective optical devices with low power consumption. The use of silicon-on-insulator (SOI) technology allows exploiting the high refractive index contrast between Si and SiO_2 (3.47 and 1.44 respectively at 1550 nm) in order to achieve high optical confinement, thus enabling the exploitation of waveguides with sub-micron dimensions and allowing curvature radii of the order of just a few microns [1]. The strong modal confinement occurring in these structures also implies that the optical intensity in these waveguides is much larger (by 2 or 3 orders of magnitude) than that in standard single-mode fibers. As a consequence, these structures have proven to be ideal candidates for all-optical signal processing thanks to highly efficient non-linear optical effects [2, 3] and, thanks to the nonlinear effects occurring in standard (220 nm high) SOI waveguides, many interesting results have already been reported in the scientific literature [4–6]. Differently from what has been thoroughly studied in the last decade, in this paper we focus our attention on reduced-height waveguides (100 nm), with different waveguide widths (from 500 to 800 nm). The interest for this particular waveguides is due to the fact that they offer promising advantages with respect to the two main limitations occurring in standard waveguides: propagation losses and nonlinear losses [7, 8]. Regarding the propagation losses it has already been reported in the literature that using reduced-height waveguides allows reducing the interaction of the optical mode with the waveguide sidewall roughness [9, 10], and as a consequence many of the integrated structures requiring low-losses (e.g. filters) are realized using reduced-height waveguides [11–13]. Regarding nonlinear impairments, the use of height-reduced waveguides allows limiting the impact of the free-carrier-absorption phenomenon, induced by two-photon-absorption when high-intensity optical beams propagate in the photonic waveguide. This is due to the fact that the recombination centers lying on waveguide surface are closer to the peak-intensity region, and so the average time required by free-carriers to reach a recombination site is significantly reduced [14].

When designing optical components for applications based on third-order optical non-linearities, an accurate knowledge of the waveguide dispersion is required to properly assess the system phase-matching bandwidth. Additionally it must be recalled that in nonlinear optical phenomena three factors mainly contribute to determine the phase-matching bandwidth: material dispersion, nonlinear chirp and waveguide geometry. At the state of the art, an experimental characterization of group index and group velocity dispersion of SOI photonic-wires realized in standard 220-SOI platform [15] or in platforms with thicker silicon layers [16, 17] has already been reported, but no experimental data are available regarding reduced-height waveguides. Additionally, it is interesting to underline that the waveguides considered in this paper were fabricated with standard CMOS processes and are then fully compatible with the multi-project-wafers protocols currently used by many institutions.

Optics EXPRESS

2. Chip structure and experimental setup

As a first step, 2D fully vectorial Finite Difference (FD) simulations using Lumerical MODE Solutions software were carried out in order to determine which is the width-range allowing to obtain single-mode propagation in the reduced-height waveguides, thus preventing polarization modal conversion and additional losses. The simulations results are showed in Fig. 1(left), where the effective indexes of the first 3 waveguide modes are plotted as a function of waveguide width.

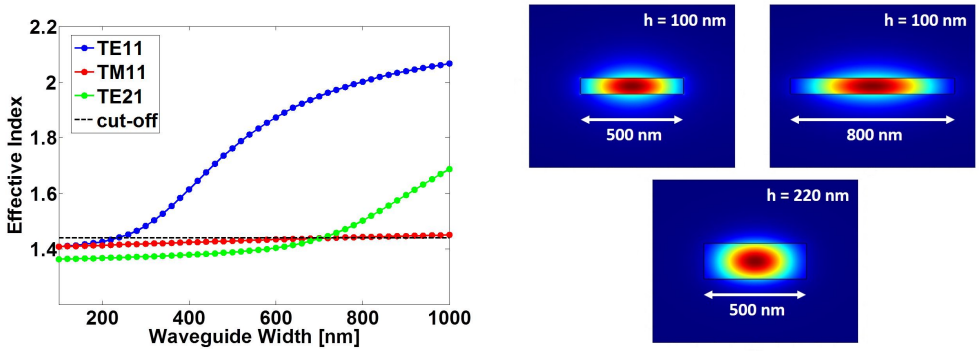

Fig. 1. (left) Simulation of the effective index of the first 3 modes of a 100 nm high waveguide at λ = 1550 nm, as a function of the waveguide width. (right) Optical power distribution in the transverse section of lowered-height and standard waveguides. The black line represents the physical cross-section of the waveguide, while the beam propagates perpendicularly to the sheet surface.

As it is can be seen from simulations, the 100 nm high waveguides support the propagation only of the fundamental TE-like mode if the width is in the range 300-700 nm, which makes the effective mode index to exceed the propagation threshold (which is basically set by the refractive index of the cladding material i.e. silicon oxide) [18]. If the waveguide is larger than ≈700 nm the second order TE-like mode is supported; anyway, even for 800-nm wide waveguide the second mode experiences high propagation and scattering losses, so that the waveguide can still be considered almost as single mode. A schematic of two lowered height waveguide cross-sections having width equal to 500 and 800 nm, superimposed with the distribution of the power density, is shown in Fig. 1(right), together with the schematic of a standard 500×220 nm strip waveguide as a comparison. In order to measure the waveguides group index, we designed a set of Mach-Zehnder interferometers (MZI) using different 100-nm high waveguides having a width of 500, 600, 700 and 800 nm respectively. We also included a structure based on the 500×220 nm waveguide, allowing us to compare our results with those already published by other groups [15]. MZIs were designed to be unbalanced, so that a significant phase difference is accumulated between light propagating in the two arms of the structure. As a result, by using a broadband source at the structure input, and analyzing the output light on an optical spectrum analyzer (OSA) a cosine-like oscillation is observed, whose free spectral range (FSR) is given by Eq. (1), where c is the speed of light in vacuum, n_g is the waveguide group index and ΔL is the length difference between the two branches of the MZI.

$$FSR = \frac{c}{n_g \Delta L} \tag{1}$$

In order to obtain a suitable FSR two different interferometers were designed, having ΔL respectively equal to 50 μm and 100 μm, for each different type of waveguide. The coupling sections of the interferometers were implemented as directional couplers, with a 300-nm gap

Optics EXPRESS

between the two waveguides. The coupling-length of each structure was calculated by 3D-FDTD numerical simulations, so as to achieve a 50% coupling at 1550 nm, and the obtained coupling-lengths varied from 7.3 to 42.2 μm. Grating couplers (1D) were designed at the input and output ports of optical waveguides and the fibers were aligned vertically on the couplers, with a tilting angle of 10 with respect to the vertical direction, in order to prevent back-reflections. The samples were fabricated at CEA-Leti Si-photonics foundry, starting from 200 mm SOI wafers, with a 2 μm thick buried oxide layer and a 220 nm thick silicon layer. The optical waveguides were patterned using 193-nm DUV lithography and two different inductively-coupled-plasma reactive-ion etching processes (ICP RIE): the first process, with an etch depth of 120 nm, was used to define the grating coupler and to lower the waveguides height from 220 nm to 100 nm, whereas the second, with a full-etch depth of 220 nm, was used to define the lateral edges of both standard and lowered-height strip waveguides. Propagation losses for the fabricated waveguides were measured to be 1.7-2 dB/cm for the 100 nm high waveguides and 2.8-3 dB/cm for the 220 nm high waveguides, thus proving that the use of reduced height waveguides can be profitable for propagation loss reduction [9, 10]. The experimental set-up used for the dispersion measurements is shown in Fig. 2. The optical source is an external cavity laser, tunable from 1475 to 1590 nm providing a maximum output power of 8 dBm and a line-width < 100 kHz. The optical beam is sent to a polarization control stage, as grating couplers on the chip are optimized for TE polarization, and then to a 99/1 power splitter: the 1% beam is used to monitor the input power, while the 99% is sent to the sample under test. The light beam is coupled back to a single mode optical fiber by means of a second grating coupler and then sent to an OSA having a resolution of 0.01 nm.

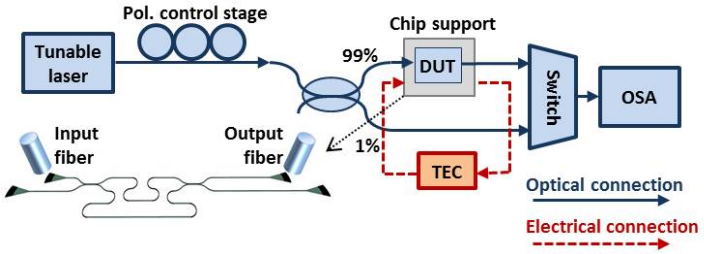

Fig. 2. Experimental setup and schematic of the MZI structure used to measure waveguides dispersion.

3. Results and discussion

Using the experimental set-up described in the previous section, measurements were performed by exploiting a 2-step procedure. At first the MZIs transfer function was recorded while sweeping the laser wavelength over its entire excursion range (1475 nm-1590 nm) with a 50-pm step. Thanks to the relatively low wavelength-resolution, the required measurement-time is limited, but the spectral ranges corresponding to the different transmission minima can be clearly extracted. The second acquisition is then performed by sweeping the laser wavelength with a 1-pm resolution over a 100-pm wide wavelength range centered around each of the previously identified minima. This procedure allows identifying the spectral position of the transmission minima with the best possible resolution on a wide wavelength range, without requiring excessive time. As an example we report in Fig. 3 the transmission function corresponding to the interferometer having a 100 μm offset ΔL between the arms, and using the 600×100 nm waveguide.

Once the spectral position of the minima in the transmission function is known, the waveguide group index n_g can be calculated by using Eq. (2), where λ_1 and λ_2 are the wavelengths corre-

Optics EXPRESS

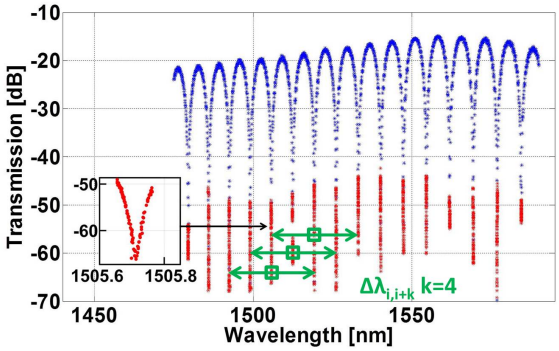

Fig. 3. Example of the experimental data acquisition. The blue dots represent the 50 pm resolution data while the red dots represents the 1 pm resolution data. The green arrows represent the wavelength windows considered (4 FSR) for the group index and dispersion calculation.

sponding to two consecutive minima. A detailed derivation of the equation, and the demonstration that the second order dispersion can be neglected in this case can be found in [19]

$$n_g = \frac{\lambda_1 \lambda_2}{\Delta L(\lambda_2 - \lambda_1)} \tag{2}$$

The group-index values obtained using Eq. (2) represent an average value of n_g in the spectral region comprised between two adjacent minima wavelengths λ_1 and λ_2. Once n_g is experimentally characterized, group velocity dispersion parameter D is calculated using Eq. (3).

$$D = \frac{1}{c} \cdot \left(\frac{dn_g}{d\lambda} \right) \tag{3}$$

In order to get reliable results for the dispersion calculation, the waveguide group index has to be measured with very high accuracy. The technique proposed in [15], where light intensity $I(\lambda)$ is used to evaluate the n_g for each wavelength point of the measured transmission spectrum, unluckily is not suitable in our situation, as the amplitude ripple due to the gratings reflections would introduce a significant noise in the n_g calculation. We therefore decided to apply a moving-average technique, and, starting from the experimental transmission spectra, we calculated the group indexes n_g by applying Eq. (2) not between two consecutive minima λ_1 and λ_2, but between two minima λ_i and λ_{i+k} separated by a k number of FSR, where k is a positive integer. In this way n_g is still calculated at each wavelength corresponding to transmission minima, but its value is now an average over a k number of FSR; an example of the wavelength windows $\Delta\lambda_{i,i+k}$ used to calculate n_g can be seen, marked by green arrows, in Fig. 3, where k is equal to 4. From Eq. (2) it can be seen that, as the error in determining λ_i and λ_{i+k} is set by the resolution of the laser source sweep (1 pm in our case), an increase of $\Delta\lambda_{i,i+k}$ will result in a reduction of the error in the n_g calculation. The measured values of n_g are reported, together with the values predicted from simulations, in Fig. 4. After having calculated n_g for different wavelengths and for each of the waveguides under test, the data points were fitted with a second order polynomial function. Finally by deriving the group-index fitting functions with respect to the optical wavelength λ, as expressed in Eq. (3), a linear expression is obtained for the dependency of the dispersion parameter D over λ. The experimental dispersion curves achieved for the different waveguide geometries and simulated dispersion curves are plotted in the left panel of Fig. 5. It is interesting to notice, see right panel of Fig. 5, that the dispersion dependence on waveguide width obtained by experimental characterization perfectly matches that expected by the 2D-FD analysis. It can

Optics EXPRESS

be seen that experimental dispersion data are in very good agreement with the theoretical model, the maximum discrepancy being equal to about ±500 ps/(nm·km) for the central wavelength of 1550 nm. It should be noticed that the difference between experimental and theoretical D values could be also due to a non perfect fabrication process, leading to small variations in the etching depth (±4% with the exploited process) or to non-ideal sidewalls verticality. Standard waveguides exhibit an anomalous D_{exp} ≈290 ps/(nm·km), which is in line with simulations D_{sim} ≈490 ps/(nm·km).

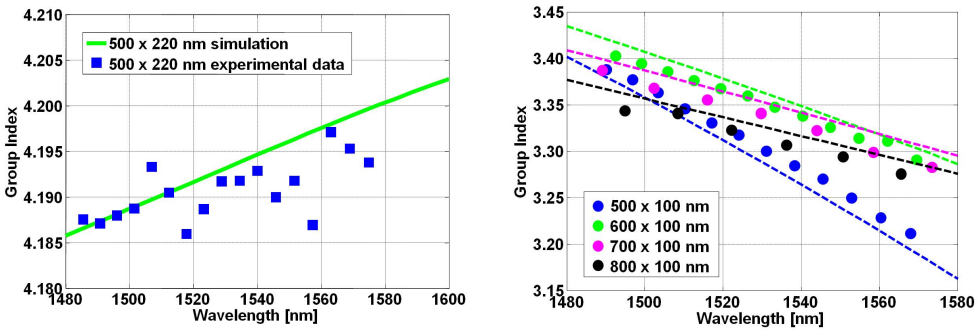

Fig. 4. (left) Experimentally derived (blue squares) group index values for standard 500x220 nm waveguides, and values predicted from simulations (green line). (right) Experimentally derived (dots) group index values for 100 nm high waveguides, and values predicted from simulations (dashed lines). Note the y-axis scale is 10 times smaller in (left) with respect to (right).

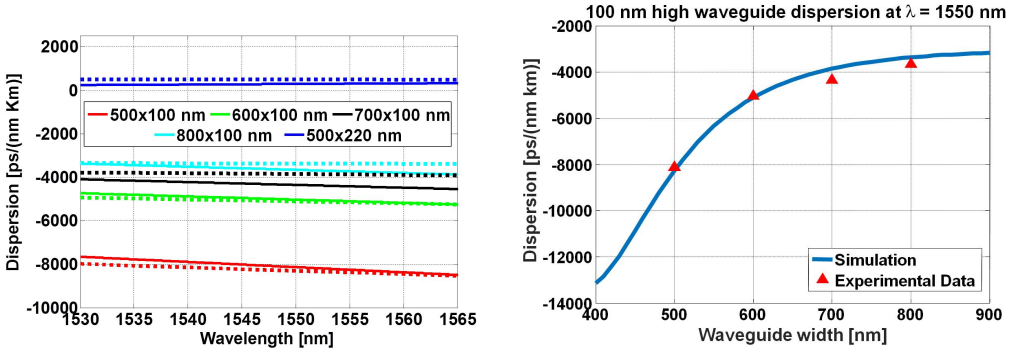

Fig. 5. (left) Dispersion curves of the analyzed waveguides in the C-band. Solid lines represent the experimentally derived curves, while dashed lines represent those derived by numerical simulations. (right) Dispersion at 1550 nm as a function of waveguide width, for 100-nm high waveguides.

The results obtained by analyzing the 100-nm high waveguides, showed that these waveguides exhibit normal dispersion. It is interesting to notice that for waveguides having a 500×100 nm cross-section the measured D parameter is -8130 ps/(nm·km) at 1550 nm, which is about 10 times bigger than the intrinsic material dispersion of silicon, D_{mat} ≈ -830 ps/(nm·km) [15], meaning that the waveguide dispersion term is the dominating one. The impact of the waveguide dispersion term is significantly reduced when the waveguide width is increased from 500 to 800 nm, as D becomes ≈ -3900 ps/(nm·km), which is significantly closer to D_{mat}.

Optics EXPRESS

4. Conclusion

In this paper we report the experimental characterization of group index n_g and optical dispersion D in reduced-height (500×100, 600×100, 700×100, and 800×100 nm) SOI strip waveguides with different widths. We confirmed the D values already reported in the literature for 500×220 nm waveguides, and obtained the first experimental data about the dispersion of reduced-height waveguides, which can be useful to the scientific community for the design of non-linear optical components. It is interesting to highlight that a large tuning of D, from -8130 ps/(nm·km) to -3900 ps/(nm·km), can be obtained by modifying waveguide width.

Funding

EU FP7-ICT-2011-8 Contract No. 318704 "FABULOUS".